

Catalytic and structural diversity of the fluazifop-inducible glutathione transferases from *Phaseolus vulgaris*

Evangelia Chronopoulou · Panagiotis Madesis ·
Basiliki Asimakopoulou · Dimitrios Platis ·
Athanasios Tsaftaris · Nikolaos E. Labrou

Received: 20 September 2011 / Accepted: 5 December 2011 / Published online: 28 December 2011
© Springer-Verlag 2011

Abstract Plant glutathione transferases (GSTs) comprise a large family of inducible enzymes that play important roles in stress tolerance and herbicide detoxification. Treatment of *Phaseolus vulgaris* leaves with the aryloxyphenoxypropionic herbicide fluazifop-*p*-butyl resulted in induction of GST activities. Three inducible GST isoenzymes were identified and separated by affinity chromatography. Their full-length cDNAs with complete open reading frame were isolated using RACE-RT and information from N-terminal amino acid sequences. Analysis of the cDNA clones showed that the deduced amino acid sequences share high homology with GSTs that belong to phi and tau classes. The three isoenzymes were expressed in *E. coli* and their substrate specificity was determined towards 20 different substrates. The results showed that the fluazifop-inducible glutathione transferases from

P. vulgaris (PvGSTs) catalyze a broad range of reactions and exhibit quite varied substrate specificity. Molecular modeling and structural analysis was used to identify key structural characteristics and to provide insights into the substrate specificity and the catalytic mechanism of these enzymes. These results provide new insights into catalytic and structural diversity of GSTs and the detoxifying mechanism used by *P. vulgaris*.

Keywords Glutathione transferase · Aryloxyphenoxypropionic herbicides · Fluazifop-*p*-butyl · Herbicide detoxification · Homology modeling

Abbreviations

AtGSTs	Glutathione transferases from <i>Arabidopsis thaliana</i>
BCNB	1-Bromo-2,4-dinitrobenzene
CDNB	1-Chloro-2,4-dinitrobenzene
CuOOH	Cumene hydroperoxide
DHAR	Dehydroascorbate
FDNB	1-Fluoro-2,4-dinitrobenzene
Fluorodifen	4-Nitrophenyl 2-nitro-4-trifluoromethylphenyl ether
Fluazifop- <i>p</i> -butyl	Butyl 2-[4-[[5-(trifluoromethyl)-2-pyridinyl]oxy]phenoxy]propanoate
G-site	Glutathione binding site
GSH	Glutathione
GST	Glutathione transferase
HED	2-Hydroxyethyl disulfide
H-site	Hydrophobic binding site
IDNB	1-Iodo-2,4-dinitrobenzene
Nb-GSH	<i>S</i> -(<i>p</i> -nitrobenzyl)-glutathione
pNPA	<i>p</i> -Nitrophenyl acetate
PvGST	Glutathione transferase from <i>Phaseolus vulgaris</i>

Electronic supplementary material The online version of this article (doi:10.1007/s00425-011-1572-z) contains supplementary material, which is available to authorized users.

E. Chronopoulou · B. Asimakopoulou · D. Platis ·
N. E. Labrou (✉)

Laboratory of Enzyme Technology, Department of Agricultural Biotechnology, Agricultural University of Athens,
75 Iera Odos Street, 11855 Athens, Greece
e-mail: lambrou@aua.gr

P. Madesis · A. Tsaftaris
Institute of Agrobiotechnology, CERTH, P.O. Box 361, 6th km
Charilaou-Thermis Road, Thessaloniki, Greece

A. Tsaftaris
Department of Genetics and Plant Breeding,
School of Agriculture, Aristotle University of Thessaloniki,
P.O. Box 261, Thessaloniki 54124, Greece

Introduction

The glutathione transferases (GSTs) are a supergene family of enzymes that catalyze the conjugation of glutathione (GSH) to reactive electrophiles. These electrophiles are diverse and include important endogenous compounds, as well as xenobiotic chemicals (Marrs 1996; Oakley 2005; McGonigle et al. 2000; Edwards and Dixon 2005; Chronopoulou and Labrou 2009). It is widely assumed that the wide substrate specificity of cytosolic GSTs correlates with structural flexibility, which allows for recognition of diverse structures at minimal energetic cost (Hou et al. 2007). In general, the catalytic efficiency of GSTs towards xenobiotics is relatively low (Armstrong 1997; Hayes et al. 2005). As in the case with other xenobiotic metabolizing enzymes (e.g., cytochrome P450, glucuronosyl transferases, etc.) low catalytic efficiency appears to be a trade-off with regard to broad substrate specificity (Koeplinger et al. 1999). Constitutive levels of GSTs are high (3–10% of total cytosolic protein) (Mannervik and Danielson 1988; Hayes and Pulford 1995) and therefore, although catalytic efficiency is relatively low, the overall detoxifying capacity is high due to the high constitutive expression (Axarli et al. 2009a).

While the majority of GST characterization has focused on mammalian forms, plants offer an exciting opportunity to examine the evolution of GSTs and their adaptive responses to biotic and abiotic stresses (e.g. herbicide treatment) (Sheehan et al. 2001; Frova 2006; Benekos et al. 2010). Metabolic detoxification is probably the major mechanism involved in plant tolerance to herbicides (Karavangeli et al. 2005; Benekos et al. 2010). It is well established that the GSH/GST system is widespread among plants and contribute to protection against herbicides by catalyzing the conjugation of glutathione to an electrophile center of herbicides. Species tolerant or susceptible to a wide spectrum of herbicides (e.g. triazines, acetanilides, thiocarbamates) are characterized by high and low levels of GSTs, respectively (Lamoureux and Rusness 1993), and an increase in specific GST activity in response to some herbicide treatment has been reported (Edwards and Cole 1996).

The plant-soluble GSTs are grouped today into seven distinct classes: phi, tau, zeta, theta, lambda, dehydroascorbate reductase, and tetrachlorohydroquinone dehalogenase classes (Edwards 1996; Droog 1997; Sheehan et al. 2001; Dixon et al. 2002a, b). The phi and tau class GSTs are specific to plants (Chronopoulou et al. 2011). Both have GSH-conjugating activities toward a diverse range of xenobiotics, including pesticides, where they are major determinants of herbicide selectivity in crops and weeds (Edwards and Dixon 2005). Different classes of herbicides such as triazines, thiocarbamates, chloroacetanilides, diphenylethers, aryloxyphenoxypropionates, etc., can be

detoxified by GSTs. Phi and tau class GSTs are induced in response to abiotic and biotic stress and play important role in counteracting oxidative stress conditions. For example, co-silencing of a group of four phi GSTs in Arabidopsis resulted in altered metabolic sensitivity to oxidative stress (Sappl et al. 2009). In addition, GSTs are also involved in the synthesis of sulfur-containing secondary metabolites such as volatiles and glucosinolates, and the conjugation, transport and storage of reactive oxylipins, phenolics and flavonoids (Dixon et al. 2010).

GSTs are usually active as a dimer of 24–29 kDa subunits with the exception of lambda class enzymes and dehydroascorbate reductases that act as monomers. Each monomer of dimeric GSTs contains a G-site capable of binding the GSH substrate and an H-site that has xenobiotic compound-binding capabilities. The G-site is mainly composed of amino acids at the N-terminal. The H-site is hydrophobic and found at the C-terminal. The H-site is less specific for substrate types allowing substrates of different and diverse structures to bind (Dixon et al. 2002a, b; Labrou et al. 2004; Chronopoulou et al. 2011).

In the present work we study the functional and catalytic diversity of selected members of the GST family from *Phaseolus vulgaris* leaves. We identified three isoenzymes that are putatively involved in the herbicide fluzifop-*p*-butyl stress response mechanism and report their cloning, kinetic characterization and structural analysis. The interest in *P. vulgaris* stems from the fact that is one of five cultivated species from the genus *Phaseolus* and is a major grain legume crop, third in importance after soybean and peanut, but first in direct human consumption (Broughton et al. 2003). Fluzifop-*p*-butyl is a selective aryloxyphenoxy propionic herbicide used for postemergence control of annual and perennial grass weeds. It is used on *Phaseolus*, soybeans and other broad-leaved crops such as carrots, spinach, potatoes, and ornamentals. Fluzifop-*p*-butyl is absorbed rapidly through leaf surfaces and quickly hydrolyzes to fluzifop acid. The acid is transported primarily in the phloem and accumulates in the meristems where it disrupts the synthesis of lipids in susceptible species (Urano 1982; Erlingson 1988) by inhibiting acetyl-CoA carboxylase.

The study of herbicide stress mechanism and detoxification systems in plants is of academic interest and practical importance. The widespread use of herbicides has led to an increasing number of resistant weed species. Herbicide resistance has the potential to cause not only large economic losses in agriculture, but also serious problems on the environment and human health, as a result of rising herbicide application rates. The lack of a basic understanding of the molecular mechanisms underlying herbicide detoxification remains the greatest obstacle to the use of eco-friendly approaches to deal with this problem.

Materials and methods

Materials

Reduced GSH, 1-chloro-2,4-dinitrobenzene (CDNB), *S*-(*p*-nitrobenzyl)-glutathione (Nb-GSH) and all other enzyme substrates were obtained from Sigma-Aldrich, USA. The pCR[®]T7/CT-TOPO[®] kit, TOPO TA Cloning[®] Kit (with pCR[®] 2.1-TOPO[®] vector), One Shot[®] Mach1[™] and SuperScript[™] II reverse transcriptase were purchased from Invitrogen, (USA). Phusion Taq DNA polymerase was purchased from FINZYMEs (Finland). Plasmid isolation kit and PCR product purification kit were purchased from Macherey–Nagel, (Germany), RNeasy Plant Mini Kit was obtained from QIAGEN, (UK), and restriction enzymes were purchased from New England Biolabs, (UK). *P. vulgaris* var. plake (florinas) was obtained from the National Agricultural Research Foundation (N.AG.RE.F.).

Methods

Plant growth

Phaseolus vulgaris seeds were pre-germinated on plates, on Whatman 2MM filter paper, (soaked in distilled water). The plates were kept for 72 h at 30°C. After germination, they were transferred into plastic pots in soil. The plants were grown in a controlled environment (12-h day/12-h night cycle, at 25°C day/21°C night regime and 65% humidity and watered with deionized water every 4 days. Plants were treated 3–4 weeks after germination having 3–4 pairs of leaves. Plants were sprayed with fluzifop-*p*-butyl (Syngenta) diluted 1/250 with deionised water (used field dose) until dripping, covered with cling film and leaf samples were collected after 24 h. Control plants were sprayed with fluzifop-*p*-butyl-free solvent, covered with cling film and leaf samples were collected after 24 h.

Purification of fluzifop-*p*-butyl-induced GSTs from *P. vulgaris* leaves

Phaseolus vulgaris leaves treated with fluzifop-*p*-butyl and control plants (non-sprayed with fluzifop-*p*-butyl plants) were used for GST purification. Protein extraction from *P. vulgaris* leaves was typically carried out by mixing leaves (5 g) with 15 mL of 50 mM sodium phosphate buffer pH 5.0. The mixture was disintegrated in a blender (total 10 min, breaking every 15 s) and placed on a rotary mixer for 60 min at 4°C. The mixture was subsequently centrifuged at 10,000g for 30 min (4°C). The supernatant was collected and passed through a 0.45 µm filter. The amount of total protein and GSTs activity was determined

by the Bradford assay and CDNB activity assay, respectively (Ayarli et al. 2009a). GSTs were isolated by affinity chromatography on GSH coupled to 1,4-butanediol diglycidyl ether-activated Sepharose (GSH-Sepharose-CL6B, 1 mL), as following: a solution of plant extract (2 mg total protein) previously dialyzed against 10 mM NaH₂PO₄, 50 mM NaCl, pH 7.0 was applied to the affinity adsorbent (1 mL). The adsorbent was washed with 10 mL of equilibration buffer. Bound proteins were eluted with equilibration buffer containing different GSH concentrations (0.1–10 mM, 2 mL). Collected fractions were analyzed by SDS-PAGE. Selected bands were electrophoretically transferred onto PVDF membranes. The bands of interest were excised from the membranes and gas-phase sequenced on the Applied Biosystems Protein Sequencer, model 477A, equipped with an on-line phenylthiohydantoin analyzer, model 120 A.

Molecular cloning

Total RNA from leaves was isolated using the RNeasy Plant Mini Kit and checked through electrophoresis for its integrity. First strand cDNA was synthesized in total volume of 20 µL by using 1–2 µg of total RNA, Superscript II was the reverse transcriptase and 500 µg RACE-RT primer 5-GGGCAACTTCTCACTCGGGTTTTTTTTTTTTTTTTTTT-3, 2 mM dNTPs, 1× superscript buffer, 100 µM DTT, 1 Unit RNaseOUT[™] and 1 Unit Superscript II enzyme (added on ice after the first step at 65°C) in a thermocycler using the following conditions 65°C for 5 min 42°C for 1 h and then 70°C for 15 min.

Amplification of the GST genes by PCR was performed with Phusion Taq DNA polymerase a specific and a nested primer for each GST gene, and the RACE AMP 5-GGGCAACTTCTCACTCGGG at the 3' end. A second PCR was performed using the nested specific primer and again the RACE AMP primer at the 3' end. We used the following conditions for all sets of primers in a total volume of 20 µL, 2 µL cDNA, 1× buffer, 5 mM dNTPs 2 µM forward and reverse primer each 1 Unit of Phusion enzyme and 12.4 µL H₂O. The program used in the thermocycler was the same for all sets of primers with the only exception being the annealing temperature for each set of primers 98°C for 30 s, 98°C 10 s, *T_m* annealing 20 s and 72°C for 30 s the programme was repeated for 35 cycles followed by a step of 72°C for 5 min. The primers used were:

PvGST2-F1 5-GAGAAAYCAAAMCATGGYASTG-3 and RACE AMP at 52°C.

PvGST3-F1 5-GGATCATCAATTCATCATATCC-3 and RACE AMP at 50°C

PvGST4-F1 5-GGAATTAGCAACTTTTCCCACG-3 and RACE AMP at 48°C

And the nested primers were PvGST2-F2 5-CAAAMCATGGYASTGAARG-3
 PvGST3-F2 5-GGAAGTGTAAAGAAAAATGGCAGAGCA-3
 PvGST4-F2 5-GGTGCTAGAGTGCTGCAATGGC-3.

The reverse primer was as before the RACE AMP and the T_m annealing for all PCR reactions was 48°C. The PCR products were analyzed on 1% agarose gel and the corresponding bands were cut out and cleaned using the NucleoSpin® Extract II according to the manufactures instructions. The clean PCR products were A-tailed using Taq polymerase and then ligated to TOPO TA Cloning® Kit (with pCR®2.1-TOPO® vector) and sequenced.

PCR was used to amplify the full-length ORFs from pCR®2.1-TOPO® vectors using the oligo primers synthesized to the 5' region of the genes from the ATG start codon and to the 3' end of the gene. The primers sequences were:

PvGST2F 5'-ATGGTAGTGAAGGTGTACGGTC-3'
 PvGST2R 5'-CTAGATTGGAGGTAGGTAGAGT-3'
 PvGST3F 5'-ATGGCAGAGCAAGAAAAGGTG-3'
 PvGST3R 5'-TCAGGCTGCAGAAGAAGATTTC-3'
 PvGST4F 5'-ATGGCTTCAAGTCAGGAAGAGG-3'
 PvGST4R 5'-CTATTTTGAAGCAAAAAGGC-3'.

The PCRs were carried out in a total volume of 50 µL that contained: 8 pmol of each primer, 1 µg template genomic DNA, 50 mM dNTPs, 5 µL 10× *Pfu* buffer and 1 Unit of *Pfu* DNA polymerase. The PCR procedure comprised 30 cycles of 2 min at 95°C, 2 min at 55°C and 2 min at 72°C. A final extension time at 72°C for 10 min was performed after the 30th cycle. The resulting PCR amplicons were TOPO ligated into a T7 expression vector (pEXP5-CT/TOPO®TA). The resulting expression constructs pT7PvGSTs were sequenced and were used to transform competent *E. coli* BL21(DE3) cells.

Expression and purification of recombinant PvGSTs

E. coli BL21(DE3) cells, harboring recombinant plasmid were grown at 37°C in 1 L LB medium containing ampicillin (100 µg/mL). The synthesis of GST was induced by the addition of 1 mM isopropyl 1-thio-β-galactopyranoside (IPTG) when the absorbance at 600 nm was 0.6. Four hours after induction, cells were harvested (approx. 3 g) by centrifugation at 8,000 rpm for 20 min, resuspended in potassium phosphate buffer (20 mM, pH 7), sonicated, and centrifuged at 13,000 rpm for 5 min. The supernatant was loaded to a column of GSH coupled to epoxy-activated Sepharose (1,4-butanediol diglycidyl ether-GSH-Sepharose-CL6B, 1 mL), which was previously equilibrated with potassium phosphate buffer (20 mM, pH 7). Non-adsorbed

protein was washed off with 10 mL equilibration buffer. Bound GST was eluted with equilibration buffer containing 10 mM glutathione. Protein purity was judged by SDS-PAGE.

Assay of enzyme activity, protein and kinetic analysis

Enzyme assays for the 1-halogen-2,4-dinitrobenzole derivatives (CDNB, FDNB, BDNB, IDNB) and fluorodifen conjugation reactions were performed according to published methods (Skopelitou et al. 2011; Axarli et al. 2009a). The electrophilic substrates were dissolved in either ethanol or acetonitrile to final concentrations of 2–5% (v/v) of the organic solvent in the assay solutions. Observed reaction velocities were corrected for spontaneous reaction rates when necessary. All initial velocities were determined in triplicate in buffers equilibrated at constant temperature. Turnover numbers were calculated on the basis of one active site per subunit. One unit of enzyme activity is defined as the amount of enzyme that catalyzes the turnover of 1 µmol of substrate per minute. Specific activity is expressed in µmol per min per mg of protein. Protein concentration was determined by the Bradford assay using bovine serum albumin (fraction V) as standard.

Steady-state kinetic measurements were performed at 37°C. Initial velocities were determined in the presence of 2.5 mM GSH and CDNB was used in the concentration range of 0.06–1.8 mM, while allyl isothiocyanate, cumene hydroperoxide and HED were used in the range of 0.3–1.2, 0.2–2 and 0.05–1.5 mM, respectively. Alternatively, these substrates were used at a fixed concentration: CDNB 1 mM, allyl isothiocyanate 0.4 mM, cumene hydroperoxide 1.5 mM and HED 2 mM while the GSH concentration was varied in the range of 0.0075–0.525 mM. Steady-state data were fitted to the Michaelis–Menten equation by nonlinear regression analysis using the GraFit (Erithacus Software Ltd.) computer program. In cases where the enzymes do not obey Michaelis–Menten kinetics the V_{max} value, $S_{0.5}$ ($S_{0.5}$ is the substrate concentration at which $v = 0.5V_{max}$), and the Hill coefficient, n_H , were determined by fitting the plotted v versus substrate concentration to the Hill equation:

$$v = \frac{V_{max} [S]^{n_H}}{S_{0.5}^{n_H} + [S]^{n_H}}$$

Curve-fits were obtained using the GraFit (Erithacus Software, Ltd.) computer program.

Difference spectroscopy

Difference spectral titrations were performed in a Perkin-Elmer Lambda16 double beam double monochromator UV–VIS spectrophotometer. Enzyme solution (1 mL; 0.5 mg

PvGSTU1-1 in 100 mM potassium phosphate, pH 6.5, containing 1 mM GSH) and enzyme solvent (1 mL; 100 mM potassium phosphate, pH 6.5, containing 1 mM GSH) were placed in the sample and reference black-wall silica cuvettes (10 mm pathlength), respectively, and the baseline difference spectrum was recorded in the range 290–600 nm. Identical volumes (2 μ L) of 1-hydroxyl-2,4-dinitrobenzene (HDNB) solution (1 mM) were added to both cuvettes and the difference spectra were recorded after each addition. The difference absorption at 355 nm was measured relative to a zero-absorbance reference area at 620 nm. The data were analyzed according to (Thompson and Stellwagen 1976; Labrou et al. 2001), using the equation:

$$\Delta A = \frac{\Delta A_{\max} [S]^{n_H}}{S_{0.5}^{n_H} + [S]^{n_H}}$$

where ΔA is the difference absorption at 355 nm after each addition of HDNB, and ΔA_{\max} is the maximum difference absorption at 355 nm at saturated concentration of HDNB.

Bioinformatics analysis and molecular modeling

GST sequences from phi, tau, zeta, theta, lambda, dehydroascorbate reductase, and tetrachlorohydroquinone dehalogenase classes and sequences homologous to PvGSTs were sought in the NCBI using pBLAST (Altschul et al. 1990). The resulting sequence set was aligned with ClustalW (Thompson et al. 1994) using BLOSUM62 as scoring matrix. ESPript (<http://esprict.ibcp.fr/ESPript/ESPript/>, Gouet et al. 1999) was used for alignment visualization and manipulation. Homology models were constructed using the program MODELLER (Sali and Blundell 1993) as implemented in UCSF Chimera (<http://www.cgl.ucsf.edu/chimera>, Pettersen et al. 2004) and five models were produced in each case. An iterative protocol

involving model constructions and rigorous protein structure quality assessment, using PROSA II (Sippl 1993), and Verify 3D (Luthy et al. 1992) was used. The available crystal structures of GSTs that were used as templates for models construction are listed in supplementary Table S1. For inspection of models and crystal structures the program PyMOL (<http://www.pymol.org/>, DeLano 2002) and UCSF Chimera were used. Coulombic surface analysis was carried out using UCSF Chimera. CastP server (<http://sts.bioengr.uic.edu/castp/calculation.php>) (Dundas et al. 2006) was used for pocket calculations using as probe radius 1.4 Å. Phylogenetic analysis was carried out using Draw-gram program (run at <http://www.phylogeny.fr/>, Dereeper et al. 2008).

Results and discussion

GST purification of the fluzafop-*p*-butyl-treated *P. vulgaris* leaves

Treatment of *P. vulgaris* leaves with fluzafop-*p*-butyl increased the total GST activity from 2.7- to 2.9-fold as assayed using 1-chloro-2,4-dinitrobenzene (CDNB) as substrate. GST activity in crude extract ranged from 0.08 to 0.12 U/mg protein, with an average of 0.1 U/mg protein ($n = 5$). Affinity chromatography on GSH-Sepharose affinity adsorbent was used to purify the GST activity from crude *P. vulgaris* leaves extracts (fluzafop-*p*-butyl-treated plants as well as control plants). The majority of the GST activity was eluted from the column in fractions between 1 and 1.75 mM using GSH as eluting agent. A separate activity was eluted from the column using salt elution (50 mM NaH₂PO₄, 1 M NaCl pH 7.5). The two distinct bands (Fig. 1) ranging in size between 24 and 26 kDa (eluted between 1 and 1.75 mM GSH) and the band eluted

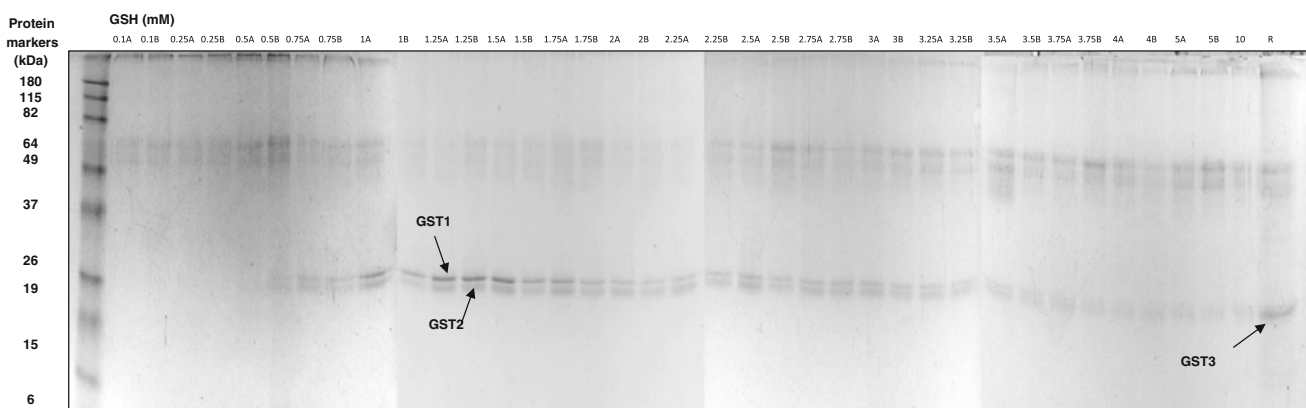


Fig. 1 SDS-PAGE analysis of GST elution profiles from the GSH-Sepharose affinity adsorbent. Separation of fluzafop-butyl-induced *P. vulgaris* GSTs by affinity chromatography on GSH-Sepharose

adsorbent. Stepwise elution was carried out using GSH (0.1–10 mM). R the fraction eluted using 50 mM NaH₂PO₄, 1 M NaCl pH 7.5

from the column using salt elution were subjected to N-terminal amino acid sequence. These bands were absent in the fractions eluted after chromatography of the extract from the control plants (data not shown). In control plants, the majority of GST activity was eluted between 2.75 and 3.75 mM GSH. N-terminal amino acid sequence of the three purified subunits gave the following sequences: MVVKVY (GST1), MAEQEK (GST2) and MASSQE (GST3).

Cloning and sequence analysis of the PvGSTs

In silico homology searches of *P. vulgaris* expressed sequence tag (EST) libraries (<http://www.ccg.unam.mx/phaseolusest/>) using as a query information the N-terminal sequences of the fluzifop-*p*-butyl-induced GSTs revealed the presence of three transcripts coding for different GSTs which were designated as GST1, GST2 and GST3. RACE-RT PCR was used to obtain the full open reading frames of GST1, GST2 and GST3. GST1, GST2 and GST3 are 696, 648, and 678 bp encoding polypeptides of 231, 215 and 225 amino acid residues, respectively. Molecular masses of the polypeptides are 26,419.60, 24,779.70 and 25,567.29 Da, with theoretical pI of 5.93, 5.84 and 5.29, respectively. All cDNAs probably represent full-length clones, as each has a stop codon present in frame downstream of the putative start methionine. In silico analysis, using iPSORT, TargetP and SignalP algorithms, revealed the absence of putative N-terminal transit peptides, suggesting that GST1, GST2 and GST3 are cytosolic enzymes.

The phylogenetic relationship of GST1, GST2 and GST3 and other GSTs from all known classes, present in public databases was investigated by the construction of a dendrogram generated by multiple amino acid sequence alignment (Fig. 2). The alignments/dendrogram were created using members of the *Arabidopsis thaliana* GST family (*At*GSTs), since *At*GSTs have been characterized in great detail and some of them are widely used as model enzymes in plant biology and stress mechanisms (Dixon et al. 2009). GST2 is clustered together with plant phi class GSTs, whereas GST1 and GST3 are clustered together with plant tau class GSTs. According to the nomenclature of Edwards et al. (2000) GST2, GST1 and GST3 may be termed as PvGSTF1-1, PvGSTU1-1 and PvGSTU2-2, respectively.

Expression, purification and substrate specificity of the recombinant enzymes

The PvGSTF1-1, PvGSTU1-1 and PvGSTU2-2 coding sequences were amplified by PCR and TOPO ligated into a T7 expression vector and the resulting expression constructs pT7PvGSTs were used to transform competent *E. coli*

BL21(DE3) cells. Recombinant PvGSTs were expressed, purified (>95% purity, data not shown) in a single-step procedure involving affinity chromatography on GSH-Sepharose and their catalytic activity was evaluated using a broad range of substrates. Purified recombinant PvGSTF1-1, PvGSTU2-2 and PvGSTU3-3 were assayed for activities as glutathione transferase, glutathione peroxidase, dehydroascorbate reductase and as thioltransferase.

The results (Table 1) showed that PvGSTs catalyze a broad range of reactions, with different members exhibiting quite varied substrate specificity. Of the several halogenated aromatic compounds that were tested, 1-chloro-2,4-dinitrobenzene (CDNB), and its analogues: 1-bromo-2,4-dinitrobenzene (BDNB), 1-fluoro-2,4-dinitrobenzene (FDNB), 1-iodo-2,4-dinitrobenzene (IDNB), and *p*-nitrobenzyl chloride (pNBC), were acceptable substrates for nearly all the enzymes although dramatic differences (~174-fold) in specific activity were observed. For example, the tau class PvGSTU2-2 exhibits the highest activity towards CDNB and its analogues, compared to the other enzymes (PvGSTF1-1 and PvGSTU1-1).

PvGSTs were also examined for glutathione-dependent peroxidase activity (GPOX) using cumene hydroperoxide, *tert*-butyl hydroperoxide, lauroyl- and benzoyl peroxides as substrates (Table 1). It is well known that GSTs participate in oxidative stress defense mechanisms by catalyzing GSH-dependent reactions that inactivate organic peroxides to the corresponding non-toxic alcohols (Bartling et al. 1993; Cummins et al. 1999). The results indicate that the tau class enzymes exhibit the highest activity towards peroxides, compared to the phi class enzyme. Among all peroxides tested cumene hydroperoxide seems to be the best substrate, whereas the bulkier substrates lauroyl- and benzoyl peroxides are not acceptable substrates for PvGSTs. Oxidative stress also results in the production of cytotoxic alkenals. One such example is *trans*-2-nonenal. *Trans*-2-nonenal is generated in the oxidation of lipids containing polyunsaturated omega-6 acyl groups, such as arachidonic or linoleic groups, and of the corresponding fatty acids (Esterbauer et al. 1986). GSTs are specifically suited to the detoxification and removal of nonenal from cells. In general, GSTs have low K_m values for nonenal catalysis and are very efficient at controlling its intracellular concentration (Balogh and Atkins 2011). Only PvGSTU2-2 showed appreciable activity towards *trans*-2-nonenal. Similarly, PvGSTs do not conjugate efficiently other alkenals substrates such *trans*-4-phenyl-3-buten-2-one, although PvGSTF1-1 and PvGSTU2-2 showed moderate activity towards ethacrynic acid. These substrates are thought to form conjugates with GSH via Michael addition reaction to the α,β -unsaturated carbonyl moiety (Labrou et al. 2004).

To determine whether PvGSTF1-1, PvGSTU1-1 and PvGSTU2-2 contribute to plant tolerance to herbicides, the

Fig. 2 a Sequence alignments (ClustalW, Thompson et al. 1994) of PvGSTF1-1, PvGSTU1-1 and PvGSTU2-2 representative members from all known GST classes: phi, tau, theta, zeta, lambda, dehydroascorbate reductase (DHAR), and tetrachlorohydroquinone dehalogenase (TCHQD). The figure was created using ESPript (Gouet et al. 1999). Conserved areas are shown shaded. A column is framed, if more than 70% of its residues are similar according to physico-chemical properties. **b** Phylogenetic analysis of PvGSTF1-1, PvGSTU1-1 and PvGSTU2-2. Phylogenetic tree was constructed the DrawGram program (run at <http://www.phylogeny.fr/>, Dereeper et al. 2008) and representative members from all known plant GST classes and PvGSTF1-1, PvGSTU1-1 and PvGSTU2-2. The cladogram was formed after alignment of the protein sequences using ClustalW. The accession numbers of GST sequences that were used were: AtGSTPhi (*Arabidopsis thaliana* phi class GST, NP_171792); AtGSTTheta (*Arabidopsis thaliana* theta class GST, NP_198937); AtDHAR (*Arabidopsis thaliana* dehydroascorbate reductase, Q9FWR4); AtGSTZeta (*Arabidopsis thaliana* zeta class GST, Q9ZVQ3); AtGSTTau (*Arabidopsis thaliana* tau class GST, AAS76278); AtGSTLambda (*Arabidopsis thaliana* lambda class GST, NP_191064); OsGSTTCHQD (*Oriza sativa* tetrachlorohydroquinone dehalogenase, CAZ68077)

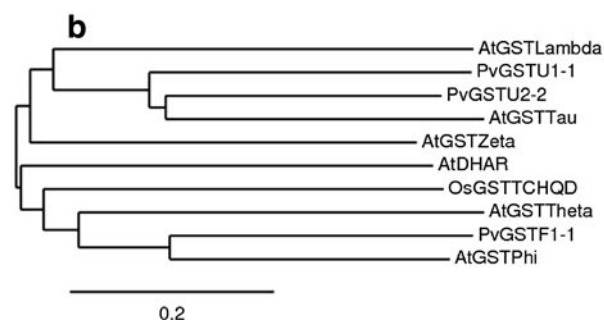
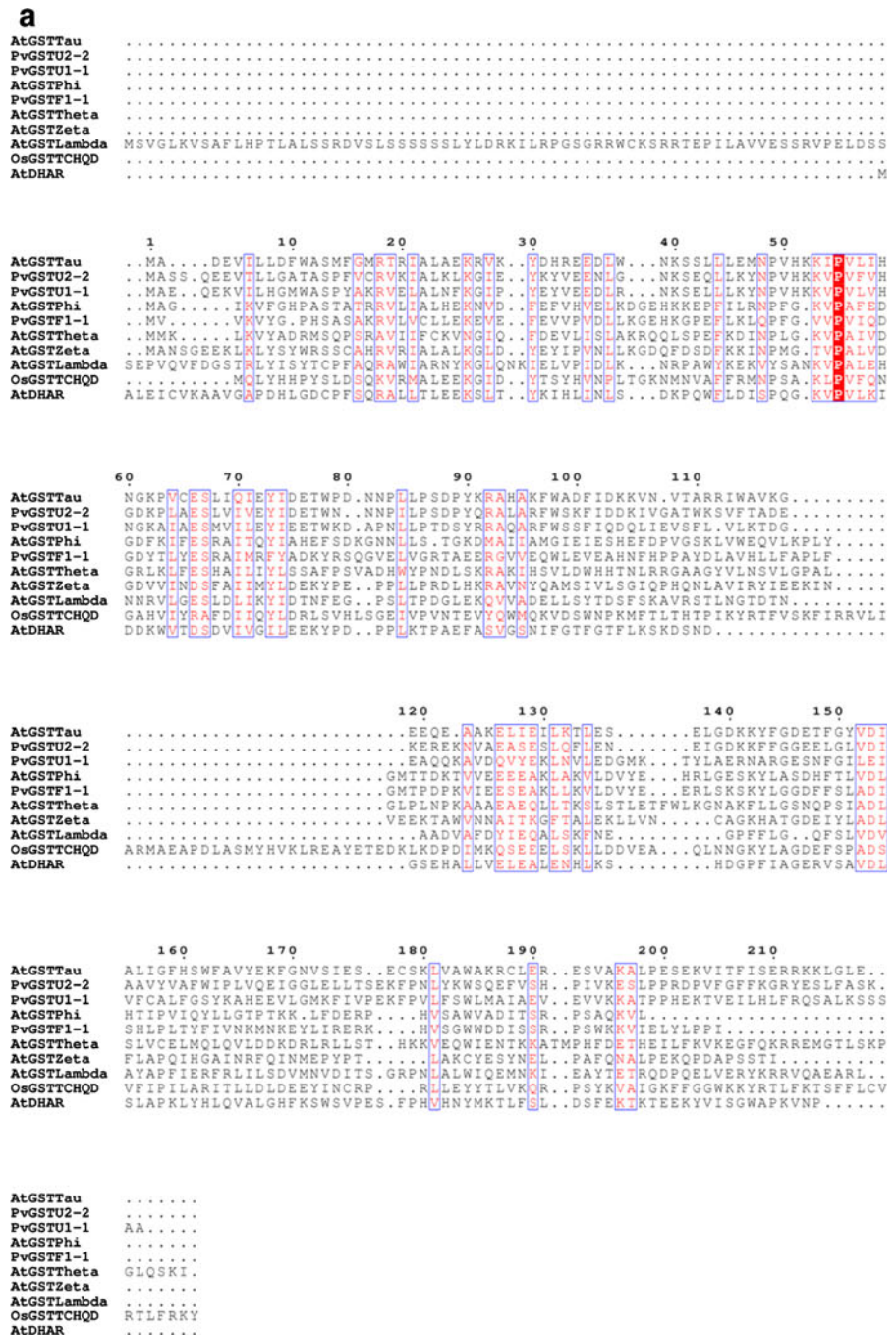


Table 1 Substrate specificity for purified recombinant *Pv*GSTF1-1, *Pv*GSTU1-1 and *Pv*GSTU2-2

Substrate	Structure	Specific activity (U/mg)		
		<i>Pv</i> GSTF1-1	<i>Pv</i> GSTU1-1	<i>Pv</i> GSTU2-2
1-Chloro-2,4-dinitrobenzene		3.5	0.28	16.6
1-Bromo-2,4-dinitrobenzene		8.4	0.64	27.9
1-Fluoro-2,4-dinitrobenzene		ND	ND	8.5
1-Iodo-2,4-dinitrobenzene		1.7	0.16	2.4
<i>p</i> -Nitrobenzyl chloride		0.70	ND	ND
4-Chloro-7-nitrobenzofurazan		3.9	0.073	148.2
Fluorodifen		ND	0.002	ND
Fluazifop- <i>p</i> -butyl		0.12	0.09	0.15
Alachlor		0.08	0.04	0.09
Metolachlor		0.03	0.01	0.05
Atrazine		0.01	0.005	0.02

Table 1 continued

Substrate	Structure	Specific activity (U/mg)		
		<i>PvGSTF1-1</i>	<i>PvGSTU1-1</i>	<i>PvGSTU2-2</i>
2,3-Dichloro-4-[2-methylenebutyryl]phenoxyacetic acid (ethacrynic acid)		2.2	ND	1.6
<i>trans</i> -4-Phenyl-3-buten-2-one		0.018	0.0008	0.57
<i>trans</i> -2-Nonenal		ND	0.009	0.13
Cumene hydroperoxide		ND	0.44	2.6
<i>tert</i> -Butyl hydroperoxide		0.015	0.071	0.54
Lauroyl peroxide		ND	ND	0.40
Benzoyl peroxide		ND	ND	ND
Allyl isothiocyanate		2.7	7.6	66.1
Phenethyl isothiocyanate		0.15	0.005	32.7
Dehydroascorbate		ND	0.013	ND
2-Hydroxyethyl disulfide (2,2-dithiodiethanol)		9.5	0.058	4.1
Bromosulphophthalein		3.6	ND	ND

Enzyme assays were carried out under standard conditions as described in “Methods” section. Results represent the means of triplicate determinations, with variation less than 5% in all cases.

ND Non-detectable

enzymes were evaluated for their ability to catalyze herbicide/GSH conjugation reactions. Table 1 shows the specific activity of the enzymes exhibited for selected herbicides that belong to phenoxy (fluzifop-*p*-butyl), triazines (atrazine), acetanilides (alachlor, metolachlor) and nitrophenyl ether herbicides (fluorodifen). All the enzymes exhibit substantial catalytic activity towards fluzifop-*p*-butyl and alachlor, moderate activity towards atrazine and metolachlor, but little or no activity toward fluorodifen. Taking into account the inducible expression of PvGSTs by fluzifop-*p*-butyl and their high catalytic activity towards fluzifop-*p*-butyl it is conceivable to assume that PvGSTs may contribute to *P. vulgaris* stress response mechanism towards fluzifop-*p*-butyl herbicide.

PvGSTs were also examined for dehydroascorbate reductase (DHAR) and thioltransferase activity (Table 1). Only PvGSTU1-1 showed very low DHAR activity catalyzing the reduction of dehydroascorbate (DHA) to ascorbic acid using GSH. A different figure was observed when PvGSTs were assayed as thioltransferases using the 2-hydroxyethyl disulfide (HED) as a substrate. PvGSTF1-1 exhibits high thioltransferase activity. This activity of PvGSTF1-1 is the most prominent among all other substrates, suggesting that this isoenzyme may play an important regulatory role. A GST-like class with DHAR activity (λ class) has already been found in *Arabidopsis* (Dixon et al. 2002a), rice and soybean (Frova 2003). These plant enzymes do not exhibit GSH-conjugating activity and unlike most other GSTs, are monomeric and form mixed disulfides with GSH (Dixon et al. 2002a). In cases of oxidative stress in the absence of GSH, some protein thiols are S-thiolated making protein-thiol disulfides. This modification is believed to play regulatory and/or protective role for protein thiols through thiolation/dethiolation reactions (Spadaro et al. 2010). The finding that PvGSTF1-1 and to a minor extent, PvGSTU2-2 are active as thioltransferase is quite interesting since so far the only plant GSTs showing this activity are the λ and DHARs (Dixon et al. 2002a, b, 2010). PvGSTF1-1 and PvGSTU2-2 appear to be the first plant GSTs to display both canonical and atypical GST functions.

PvGSTs catalyze (Table 1) the addition of the thiol group of GSH to the electrophilic central carbon of the isothiocyanate group (using allyl isothiocyanate and phenethyl isothiocyanate as substrates) to form dithiocarbamates [R-NH-C(=S)-SG] (Meyer et al. 1995). In general, the aliphatic allyl-isothiocyanate was a better substrate for PvGSTs, compared to the bulkier phenylethyl-isothiocyanate. Isothiocyanates are abundant in a variety of edible vegetables (Kolm et al. 1995). Allyl-isothiocyanate serves as a defense against herbivores; since it is harmful to the plant itself, it is stored in the harmless form of the glucosinolate (Agrawal and Kurashige 2003).

Kinetic analysis

Steady-state kinetic analysis for the model substrate CDNB was carried out and the k_{cat} and K_m parameters were determined (Table 2). PvGSTF1-1 and PvGSTU2-2 obey Michaelis–Menten kinetics. The K_m values of PvGSTF1-1 and PvGSTU2-2 for CDNB, fall within the range for plant GSTs (Labrou et al. 2004; Axarli et al. 2009a, b). The PvGSTF1-1 and PvGSTU2-2 k_m values for GSH is about 5–10 times lower compared to that observed for other plant isoenzymes (Labrou et al. 2004; Axarli et al. 2009a, b). On the other hand, PvGSTU1-1 does not obey Michaelis–Menten kinetics using CDNB as a variable substrate. Steady-state kinetic analysis of PvGSTU1-1 showed that when CDNB was used as a variable substrate with GSH at fixed concentration, a sigmoid substrate dependence was observed (Fig. 3). Data of initial velocities were well fitted to a rate equation expressing positive cooperativity between the two H-sites. On the other hand, when GSH was used as a variable substrate with CDNB at fixed concentration, a Michaelis–Menten hyperbolic dependence was observed. The kinetic parameters k_{cat} , K_m^{GSH} , $S_{0.5}^{CDNB}$ and n_H were determined by steady-state kinetic analysis and the results are listed in Table 3. A different kinetic behavior was observed using allyl-isothiocyanate/GSH as substrate system. When allyl-isothiocyanate was used as a variable substrate with GSH at fixed concentration, and when GSH was used as a variable substrate with allyl-isothiocyanate at fixed concentration a sigmoid dependence

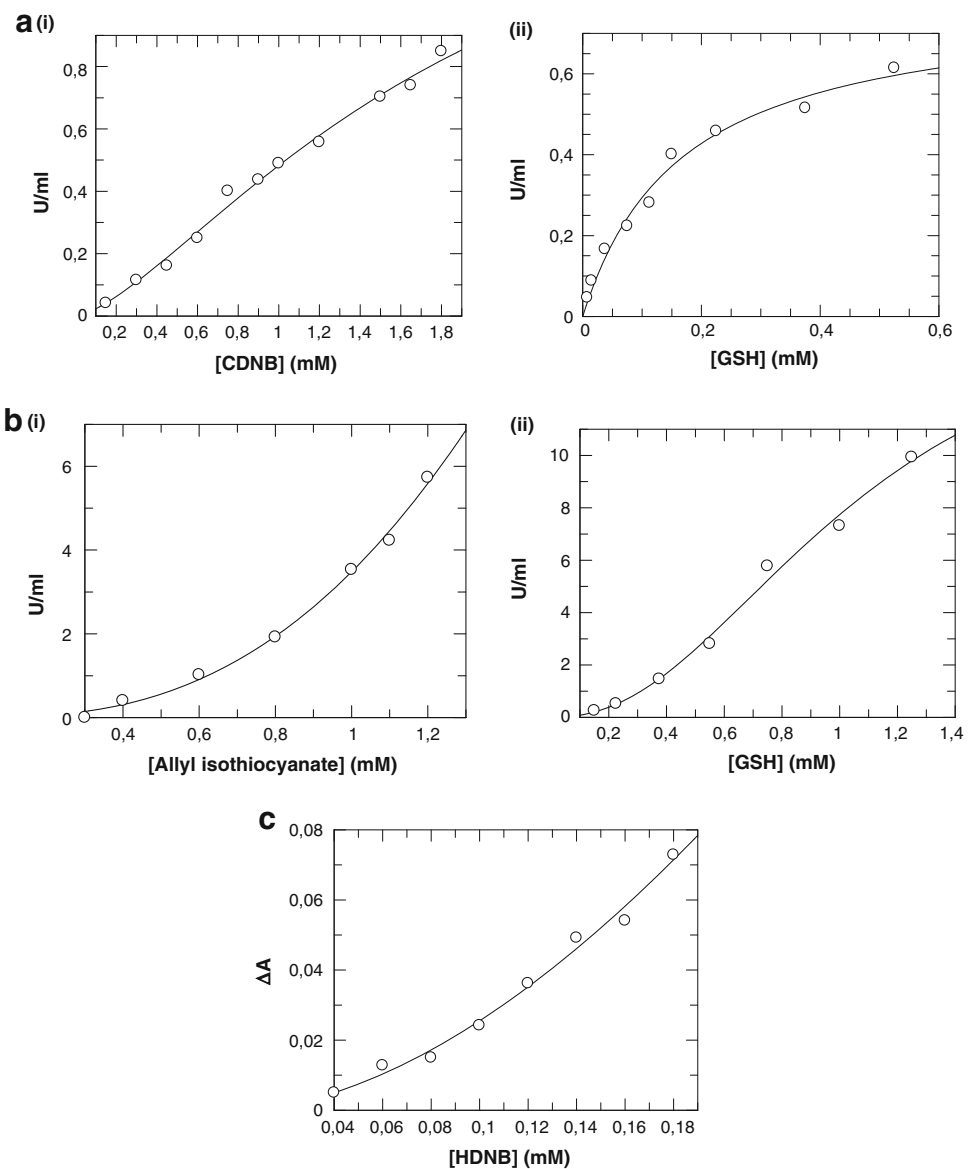
Table 2 Steady-state kinetic analysis of PvGSTF1-1 and PvGSTU2-2 for the CDNB/GSH substrate system

Electrophilic substrate/enzyme	K_m (μM) (GSH)	k_{cat} (min^{-1}) (GSH)	K_m (μM) (CDNB)	k_{cat} (min^{-1}) (CDNB)	k_{cat}/K_m ($\mu\text{M}^{-1} \text{min}^{-1}$) (GSH)	k_{cat}/K_m ($\mu\text{M}^{-1} \text{min}^{-1}$) (CDNB)
PvGSTF1-1	44.4 \pm 3.4	17.5 \pm 0.339	5,873.7 \pm 2,391.2	412.4 \pm 165.5	0.395 \pm 0.0227	0.0074 \pm 0.004
PvGSTU1-1	167.3 \pm 26.4	5.038 \pm 0.335	ND	ND	0.155 \pm 0.122	ND
PvGSTU2-2	49.6 \pm 6.2	650.4 \pm 19.165	864.6 \pm 110.8	1,274 \pm 80.61	13.271 \pm 1.272	1.485 \pm 0.0975

PvGSTU1-1 does not obey Michaelis–Menden kinetics using CDNB as a variable substrate in the GSH/CDNB system (see Table 3)

ND Not determined

Fig. 3 **a** Kinetic analysis of *PvGSTU1-1* using the CDNB as a variable substrate **(i)** and GSH at a fixed concentration. Kinetic analysis of *PvGSTU1-1* using the GSH as variable substrate **(ii)** and CDNB at a fixed concentration. **b** Kinetic analysis of *PvGSTU1-1* using the allyl-isothiocyanate as a variable substrate **(i)** and GSH at a fixed concentration. Kinetic analysis of *PvGSTU1-1* using the GSH as variable substrate **(ii)** and allyl-isothiocyanate at a fixed concentration. Experiments were performed in triplicate and lines were that calculated by least-squares regression analysis. **c** Spectroscopic analysis of HDNB binding to *PvGSTU1-1*. The graph shows the difference absorbance at 310 nm as a function of the total HDNB concentration



were observed for both substrates (Fig. 3). Data of initial velocities were well fitted to a rate equation expressing positive cooperativity between the two H-sites and G-sites and the kinetic parameters k_{cat} , $S_{0.5}^{GSH}$, $S_{0.5}^{allyl\ isothiocyanate}$ and n_H are listed in Table 3. It is noteworthy that the enzymes *PvGSTU1-1* and *PvGSTF1-1* exhibit normal hyperbolic Michaelis–Menten kinetics toward the substrates systems CuOOH/GSH and HED/GSH. For example, for *PvGSTU1-1* (CuOOH/GSH system) k_{cat} was determined to be equal to $19.9 \pm 5.9\ \text{min}^{-1}$ and the K_m parameters were $7,780 \pm 285\ \mu\text{M}$ (for CuOOH) and $5,224 \pm 3,697\ \mu\text{M}$ (for GSH). For *PvGSTF1-1* (HED/GSH system) the k_{cat} was equal to $10.8 \pm 0.4\ \text{min}^{-1}$ and K_m values $131.3 \pm 20.4\ \mu\text{M}$ (for HED) and $3,216.7 \pm 689.7\ \mu\text{M}$ (for GSH).

The apparent positive cooperativity observed for *PvGSTU1-1* has several possible sources (Ricci et al. 1995; Lo Bello et al. 1995; Labrou et al. 2001). One possibility is

that the enzyme follows a steady-state random kinetic scheme (Labrou et al. 2001). A dimeric enzyme which has two independent subunits and two substrates may, under certain conditions, show apparent positive cooperativity if it follows a steady-state random mechanism (Segel 1975). For example, the non-Michaelian kinetic behavior of *Lucilia cuprina* GST (Caccuri et al. 1997) rat GSTs M1-1, M1-2 and A3-3 (Ivanetich et al. 1990; Jakobson et al. 1979), has been explained as a result of steady-state random sequential Bi Bi mechanism. Another source of apparent cooperativity may be a substrate-induced change of the dimer–tetramer equilibrium as observed in *Plasmodium falciparum* GST (Liebau et al. 2009). The third possibility is that the substrate (CDNB or allyl-isothiocyanate) binding to the first subunit induces a conformational change in the second subunit which therefore displays an increased affinity for the substrate (Ricci et al. 1995; Lo

Table 3 Steady-state kinetic analysis of PvGSTU1-1 for the CDNB/GSH and allyl-isothiocyanate/GSH substrate systems

Substrates	Kinetic parameters	GSH	CDNB or allyl-isothiocyanate
CDNB/GSH	k_{cat}	ND	10.8 ± 3.5
	$S_{0.5}^{\text{CDNB}}$	ND	2.5 ± 1.2
	n_{H}	ND	1.5 ± 0.2
Allyl-isothiocyanate/GSH	k_{cat}	105.9 ± 32.8	37.4
	$S_{0.5}^{\text{GSH}}$	1.1 ± 0.7	–
	$S_{0.5}^{\text{Allyl isothiocyanate}}$	–	5.8
	n_{H}	2.2 ± 0.4	1.7

PvGSTU1-1 obeys Michaelis–Menten kinetics using GSH as a variable substrate in the GSH/CDNB system (see Table 2)

ND Not determined

Bello et al. 1995; McManus et al. 2011). To distinguish between these possibilities, we analyzed the isothermic binding of 1-hydroxy-2,4-dinitrobenzene (the hydrolysed product of CDNB) to the PvGSTU1-1 in the presence of GSH using UV difference spectroscopy (Fig. 3). The enzyme exhibited a sigmoidal isothermic binding curve (Fig. 3) with Hill coefficient of 1.6 ± 0.1 , very close to that found with the kinetic procedure. These results support the idea of true cooperative binding and rule out the possibility that the cooperativity is due to a steady-state random mechanism. The Hill coefficients obtained by difference spectroscopy (performed at 0.5 mg/mL protein) and by kinetic analysis (performed at 0.5 $\mu\text{g/mL}$ protein, Table 3) are similar, therefore making less likely the involvement of any monomer–dimer equilibrium in the positive cooperativity for CDNB binding seen for the PvGSTU1-1 enzyme.

The actual role of the positive cooperation that was observed is not fully understood. GSTs provide an impressive catalytic potential for the metabolism and elimination of any potential toxin to which the cell may be exposed and presumably the allosteric kinetic behavior provides a detoxification advantage when bioactivated toxic products are a significant threat (Atkins et al. 2002; McManus et al. 2011). Allyl isothiocyanate is a toxic organosulfur compound that serves the plant as a defense against herbivores. Since it is harmful to the plant itself, it is stored in the harmless form of the glucosinolate. The enzyme myrosinase acts on a glucosinolate to give allyl isothiocyanate. At low allyl isothiocyanate concentrations, the slower substrate turnover achieved by a cooperative enzyme (e.g. PvGSTU1-1) compared to an enzyme that obeys Michaelis–Menten kinetics can be a significant toxicological advantage, when toxic thresholds exist thus minimizing the possibility to exceed its toxic threshold. The high substrate turnover achieved by a non-cooperative

enzyme may be a disadvantage for an organism to quickly convert substrate at concentration under the toxic threshold. The positive homotropic allosteric enzymes can minimize this disadvantage. At high allyl isothiocyanate concentrations associated with a high probability of toxicity, fast turnover is desirable, and this advantage is provided by the cooperative enzymes. The positive homotropic cooperativity that is observed for allyl isothiocyanate is achieved without other specific molecular recognition that can be an advantage for the cell (Atkins et al. 2002).

Molecular modeling

To understand the catalytic and structural properties of PvGSTF1-1, PvGSTU1-1 and PvGSTU2-2 the enzymes were subjected to structural determination by homology modeling. The three-dimensional structure of PvGSTF1-1, PvGSTU1-1 and PvGSTU2-2 were modeled based on X-ray structures of plant GSTs (Table S1; Fig. 4). Total monomer surface area for PvGSTF1-1, PvGSTU1-1 and PvGSTU2-2 are calculated equal to 9,868, 9,604 and 9,460 \AA^2 , respectively. The three PvGSTs shared the same structure pattern (Figs. 4, 5). Each monomer of PvGSTs constitutes two distinct domains; a smaller thioredoxin-like N-terminal domain and a larger helical C-terminal domain. The N-terminal small domain is an α/β structure with the folding topology $\beta\alpha\beta\alpha\beta\beta\alpha$ arranged in the order $\beta 2$, $\beta 1$, $\beta 3$ and $\beta 4$ with $\beta 3$ anti-parallel to the others, forming a regular β -sheet with a right-handed twist surrounded by three α -helices. At the end of helix H3 begins a short linker that joins the N- and C-terminal domains. The core of the C-terminal domain is a bundle of four helices (H4H5H6H7). Comparison of the structure of the phi class PvGSTF1-1 with PvGSTU1-1 and PvGSTU2-2 reveals that the central four-stranded β -sheet and the up and down arrangement of helices H4 and H5 are very similar. Discrepancies are observed in the linker segment, the C-terminal region and the region of the helix joining strands $\beta 2$ and $\beta 3$. A significant variation with respect to the *A. thaliana* phi class enzyme structure (Reinemer et al. 1996) was observed in the region following H8, which differs remarkably in length and sequence/conformation.

The active site of PvGSTU1-1 and PvGSTU2-2 appears as a large inverted L-shape which is different in shape and size from PvGSTF1-1 which has a large and open cavity. Active site solvent accessible surface (Richards' surface) for PvGSTF1-1, PvGSTU1-1 and PvGSTU2-2 has been calculated equal to 345.7, 722.5 and 334.6 \AA^2 , respectively. The residues involved in the formation of G-site (GSH-binding site) binding pocket are given in Table 4. The GSH moiety of the bound molecule is located in a polar region, formed by the beginning of helices H1, H2

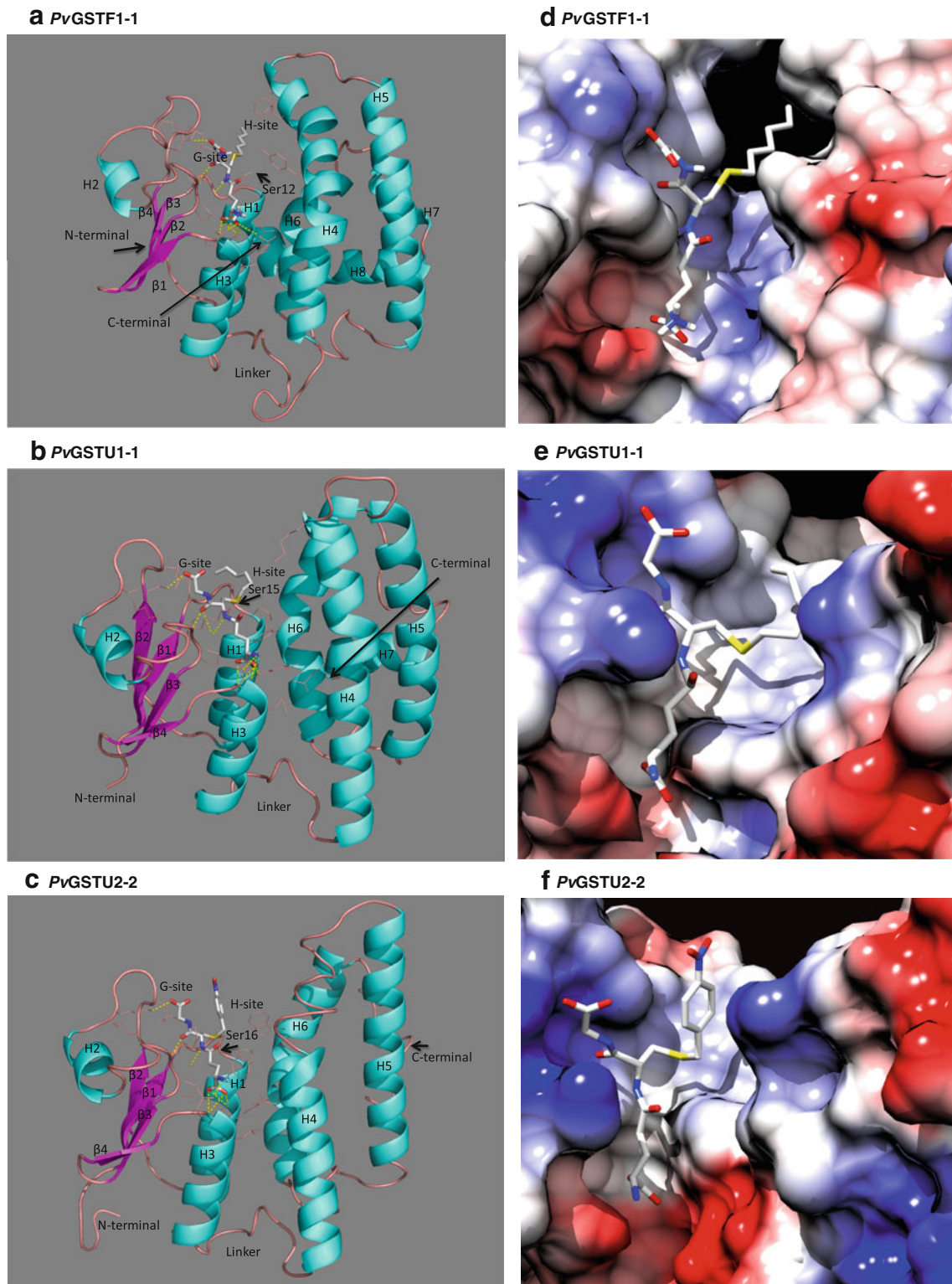


Fig. 4 Ribbon diagrams of *PvGSTF1-1* (a), *PvGSTU1-1* (b) and *PvGSTU2-2* (c) protein models. Helices (*H*) are in turquoise and β -strands (β) in magenta. The GSH analogues (*S*-hexyl-GSH for *PvGSTF1-1* and *PvGSTU1-1* and *p*-nitrobenzyl-GSH for *PvGSTU2-2*) are represented in a stick and colored according to atom type. The location of active site Ser residue, the G- and H-site as well as the

C-, and N-terminal and the linker are labeled. The molecular figures were created using PyMOL (DeLano 2002). Coulombic surface analysis of *PvGSTF1-1* (d), *PvGSTU1-1* (e) and *PvGSTU2-2* (f). The analysis was carried out using UCSF Chimera (<http://www.cgl.ucsf.edu/chimera>). The Coulomb electrostatic surface shows regions of neutral (white), positive (blue) and negative (red) charge

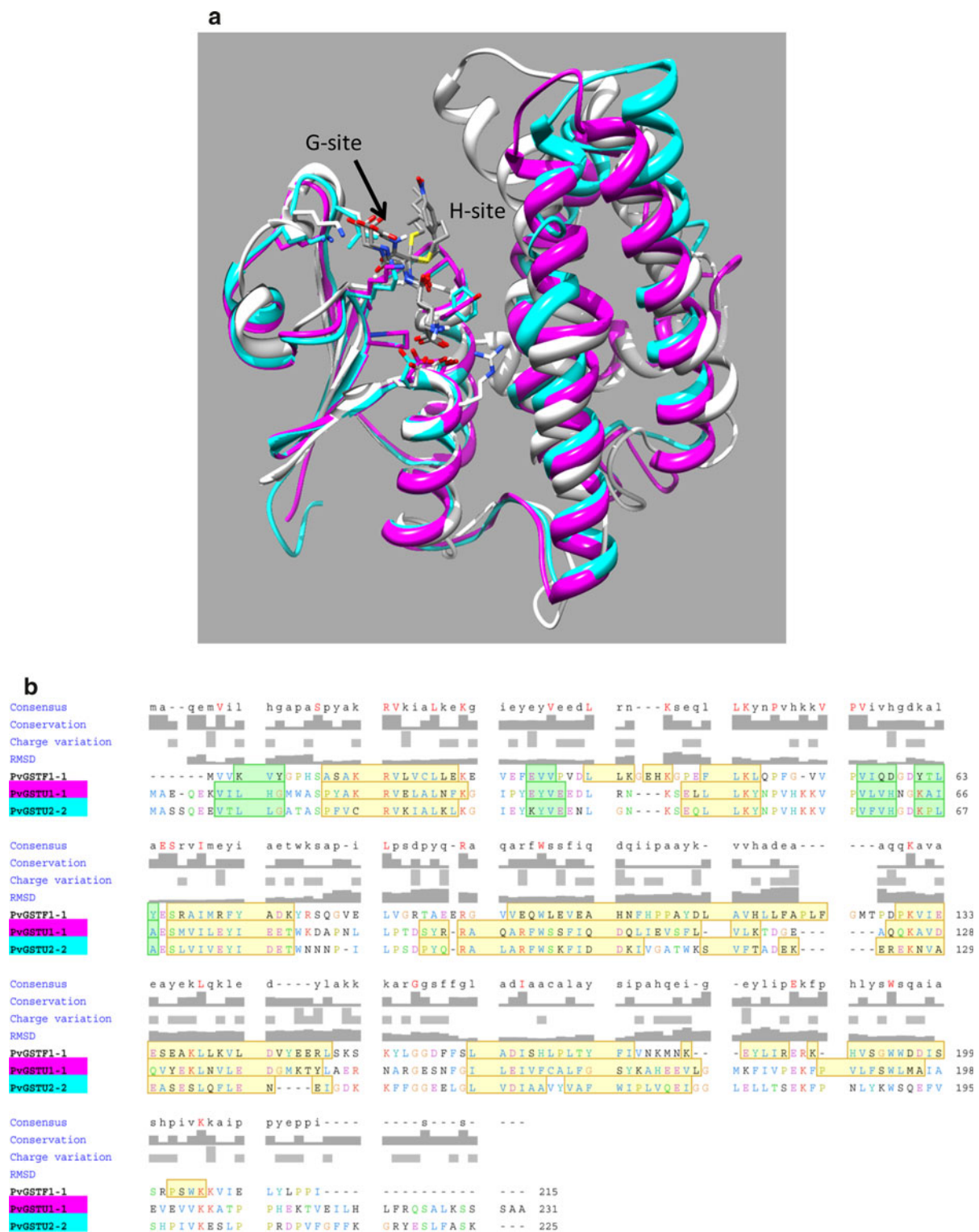


Fig. 5 a Structural alignments of PvGSTF1-1 (white), PvGSTU1-1 (magenta) and PvGSTU2-2 (turquoise) protein models. The analysis was carried out using UCSF Chimera (<http://www.cgl.ucsf.edu/chimera>). **b** Structure-based sequence alignment of the homology models. Light green and orange depict regions of β -strands and

α -helices, respectively. Numbering for each model is shown on the right of the sequence. Residue coloring is based on Clustal X one-letter residue coloring. The analysis was carried out using UCSF Chimera (<http://www.cgl.ucsf.edu/chimera>)

and H3 in the N-terminal domain. The SNAIL/TRAIL-like motif (Pemble et al. 1996) in the N-terminal domain that is present in most GST classes and contributes polar functional groups to the GSH-binding site, located in the dimer interface is found in all *Pv*GSTs. SNAIL/TRAIL-like motifs were found at amino acids positions 66–90 (*Pv*GSTF1-1 numbering, Fig. 5b) with some modifications.

Coulombic surface analysis (Fig. 4) showed that the G-site in the tau class enzymes (*Pv*GSTU1-1 and *Pv*GSTU2-2) shows much more positive electrostatic potential compared to *Pv*GSTF1-1. This positive electrostatic potential of the G-site may contribute to -SH ionization of GSH (Labrou et al. 2001). The involvement of positively charged residues in the electrostatic field regulation has also been observed in other GSTs (Patskovsky et al. 2000). There is no direct interaction between the GSH moiety and residues of the C-terminal domain. It is well established that the plant tau and phi class enzymes possess as a catalytic residue Ser (Labrou et al. 2001; Axarli et al. 2009a, b). Analysis of *Pv*GSTF1-1, *Pv*GSTU1-1 and *Pv*GSTU2-2 modeled structures shows that there is one Ser residue that could be catalytically important: Ser12 (distance from the S atom of GSH 2.9 Å), Ser15 (distance from the S atom of GSH 3.1 Å), Ser16 (distance from the S atom of GSH 3.3 Å) in *Pv*GSTF1-1, *Pv*GSTU1-1 and *Pv*GSTU2-2, respectively.

The H-site of *Pv*GSTF1-1, *Pv*GSTU1-1 and *Pv*GSTU2-2 is located next to the G-site and is formed by hydrophobic residues from the C-terminal domain. The H-sites of *Pv*GSTs exhibit a low degree of sequence identity and hence a unique structure that reflects their different substrate specificity (Fig. 5). The H-site of *Pv*GSTF1-1 is more hydrophobic in nature and exposed to the bulk solvent compared to the H-sites of *Pv*GSTU1-1 and *Pv*GSTU2-2 (Fig. 5b). In *Pv*GSTU1-1 and *Pv*GSTU2-2 positively charged residues (e.g. Lys117, Lys55 in *Pv*GSTU1-1) make the approach to the H-site basic. These basic residues form a positively charged region at the H-site, which presumably enable the enzyme to bind negatively charged substrates.

The C-terminal domain of cytosolic GSTs contains a strictly conserved N-capping box motif (Ser/Thr-Xaa-Xaa-Asp) at the beginning of H6 in the hydrophobic core of the molecule (Cocco et al. 2001). In GSTs, the N-capping box is involved in the H6-helix formation, plays crucial structural and functional roles and is essential to the folding of GSTs. The N-capping box consists of a hydrogen bonding interaction of the hydroxyl group of Ser/Thr with Asp (Aceto et al. 1997). Interestingly, only *Pv*GSTF1-1 possesses a conserved N-capping box motif (Ser-Leu-Ala-Asp) that is located between amino acids 162 and 165. In tau class *Pv*GSTU1-1 and *Pv*GSTU2-2 the respective sequences are Gly-Ile-Leu-Glu and Gly-Leu-Val-Asp, suggesting the absence of the critical hydrogen bonding interaction

Table 4 Amino acid residue that participate in G-site formation

Enzyme	Amino acids
<i>Pv</i> GSTF1-1	Ser12, Leu34, His39, Lys40m Val52, Val53, Glu65, Ser66
<i>Pv</i> GSTU1-1	Ser15, Tyr17, Leu39, Lys42, Lys55, Val56, Pro57, Glu68, Ser69
<i>Pv</i> GSTU2-2	Ser16, Phe18, Leu40, Lys43, Lys56, Val57, Glu69, Ser70

Analysis was carried out using What IF

between Ser and Asp. This indicates that the folding mechanism of tau class GSTs may be different compared to phi class GSTs.

Conclusions

In the present work, we describe the characterization of three fluzafop-inducible GSTs from *P. vulgaris*. The results showed that *Pv*GSTs are capable of catalyzing several different reactions and substrates, including herbicides, and exhibit wide substrate specificity. Structural analysis showed that *Pv*GSTs share the same overall fold and domain organization of other plant cytosolic GSTs, with major differences at their active site and some differences at the level of C-terminal domain and the linker between the C- and N-terminal domains. The structural heterogeneity within the C-terminal domain seems to be responsible for the substrate variability and specificity across *Pv*GSTs. Taking into account the inducible expression of *Pv*GSTs by fluzafop-*p*-butyl and their high catalytic activity towards fluzafop-*p*-butyl, it is conceivable to assume that *Pv*GSTs may contribute to *P. vulgaris* stress response mechanism towards fluzafop-*p*-butyl. The methodology reported in the present study for the discovery of novel enzymes involved in herbicide stress response may find applications in other plant/stress systems.

Acknowledgments The authors thank the Ministry of Education, Lifelong Learning and Religious Affairs for the financial assistance provided. This work was performed within the grants HRAKLEITOS II (the grant was awarded to E.C. and N.E.L.) and THALES. These actions fall under the Operational Programme “Education and Lifelong Learning” and are co-funded by the European Social Fund and National Resources.

References

- Aceto A, Dragani B, Melino S, Allocati N, Masulli M, Di Ilio C, Petruzzelli R (1997) Identification of an N-capping box that affects the α 6-helix propensity in glutathione S-transferase superfamily proteins: a role for an invariant aspartic residue. *Biochem J* 322:229–234

- Agrawal AA, Kurashige NS (2003) A role for isothiocyanates in plant resistance against the specialist herbivore *Pieris rapae*. *J Chem Ecol* 29:1403–1415
- Altschul SF, Gish W, Miller W, Myers EW, Lipman DJ (1990) Basic local alignment search tool. *J Mol Biol* 215:403–410
- Armstrong RN (1997) Structure, catalytic mechanism, and evolution of the glutathione transferases. *Chem Res Toxicol* 10:2–18
- Atkins WM, Lu WD, Cook DL (2002) Is there a toxicological advantage for non-hyperbolic kinetics in cytochrome P450 catalysis? Functional allostery from “distributive catalysis”. *J Biol Chem* 277:33258–33266
- Axarli I, Dhavala P, Papageorgiou AC, Labrou NE (2009a) Crystallographic and functional characterization of the fluorodifen-inducible glutathione transferase from *Glycine max* reveals an active site topography suited for diphenylether herbicides and a novel L-site. *J Mol Biol* 385:984–1002
- Axarli I, Dhavala P, Papageorgiou AC, Labrou NE (2009b) Crystal structure of *Glycine max* glutathione transferase in complex with glutathione: investigation of the mechanism operating by the Tau class glutathione transferases. *Biochem J* 422:247–256
- Balogh LM, Atkins WM (2011) Interactions of glutathione transferases with 4-hydroxynonenal. *Drug Metab Rev* 43:165–178
- Bartling D, Radzio R, Steiner U, Weiler EW (1993) A glutathione S-transferase with glutathione-peroxidase activity from *Arabidopsis thaliana*. Molecular cloning and functional characterization. *Eur J Biochem* 216:579–586
- Benekos K, Kissoudis C, Nianiou-Obeidat I, Labrou N, Madesis P, Kalamaki M, Makris A, Tsaftaris A (2010) Overexpression of a specific soybean GmGSTU4 isoenzyme improves diphenyl ether and chloroacetanilide herbicide tolerance of transgenic tobacco plants. *J Biotechnol* 150:195–201
- Broughton WJ, Hernandez G, Blair MW, Beebe SE, Gepts P, Vanderleyden J (2003) Beans (*Phaseolus* spp.)—model food legumes. *Plant Soil* 252:55–128
- Caccuri A, Antonini G, Nicotra M, Battistoni A, Lo Bello M, Board P, Parker M, Ricci G (1997) Catalytic mechanism and role of hydroxyl residues in the active site of theta class glutathione S-transferases. Investigation of Ser-9 and Tyr-113 in a glutathione S-transferase from the Australian sheep blowfly, *Lucilia cuprina*. *J Biol Chem* 274:29681–29686
- Chronopoulou EG, Labrou NE (2009) Glutathione transferases: emerging multidisciplinary tools in red and green biotechnology. *Recent Pat Biotechnol* 3:211–223
- Chronopoulou E, Axarli I, Nianiou-Obeidat I, Madesis P, Tsaftaris A, Labrou NE (2011) Structure and antioxidant catalytic function of plant glutathione transferases. *Curr Chem Biol* 5:64–74
- Cocco R, Stenberg G, Dragani B, Rossi Principe D, Paludi D, Mannervik B, Aceto A (2001) The folding and stability of human alpha class glutathione transferase A1-1 depend on distinct roles of a conserved N-capping box and hydrophobic staple motif. *J Biol Chem* 276:32177–32183
- Cummins I, Cole DJ, Edwards R (1999) A role for glutathione transferases functioning as glutathione peroxidases in resistance to multiple herbicides in black-grass. *Plant J* 18:285–292
- DeLano WL (2002) The PyMOL Molecular Graphics System DeLano Scientific. San Carlos, CA, USA
- Dereeper A, Guignon V, Blanc G, Audic S, Buffet S, Chevenet F, Dufayard JF, Guindon S, Lefort V, Lescot M, Claverie JM, Gascuel O (2008) Phylogeny.fr: robust phylogenetic analysis for the non-specialist. *Nucleic Acids Res* 36:W465–W469
- Dixon DP, Davis BG, Edwards R (2002a) Functional divergence in the glutathione transferase superfamily in plants. Identification of two classes with putative functions in redox homeostasis in *Arabidopsis thaliana*. *J Biol Chem* 277:30859–30869
- Dixon DP, Laphorn A, Edwards R (2002b) Protein family review: plant glutathione transferases. *Genome Biol* 3:3004.1–3004.10
- Dixon DP, Hawkins T, Hussey PJ, Edwards R (2009) Enzyme activities and subcellular localization of members of the Arabidopsis glutathione transferase superfamily. *J Exp Bot* 60:1207–1218
- Dixon DP, Skipsey M, Edwards R (2010) Roles for glutathione transferases in plant secondary metabolism. *Phytochemistry* 71:338–350
- Droog F (1997) Plant glutathione S-Transferases, a tale of theta and tau. *J Plant Growth Regul* 16:95–107
- Dundas J, Ouyang Z, Tseng J, Binkowski A, Turpaz Y, Liang J (2006) CASTp: computed atlas of surface topography of proteins with structural and topographical mapping of functionally annotated residues. *Nucleic Acids Res* 34:W116–W118
- Edwards R (1996) Characterisation of glutathione transferases and glutathione peroxidases in pea (*Pisum sativum*). *Physiol Plant* 98:594–604
- Edwards R, Cole DG (1996) Glutathione transferases in wheat (*Triticum*) species with activity toward fenoxaprop-ethyl and other herbicides. *Pestic Biochem Physiol* 54:96–104
- Edwards R, Dixon DP (2005) Plant glutathione transferases. *Methods Enzymol* 401:169–186
- Edwards R, Dixon DP, Walbot V (2000) Plant glutathione S-transferases: enzymes with multiple functions in sickness and in health. *Trends Plant Sci* 5:193–198
- Erlingsson M (1988) Fusilade—a strategy for long-term control of couch (*Elymus repens*). *Weeds Weed Control* 1:158–165
- Esterbauer H, Benedetti A, Lang J, Fulceri R, Fauler G, Comporti M (1986) Studies on the mechanism of formation of 4-hydroxynonenal during microsomal lipid peroxidation. *Biochim Biophys Acta* 876:154–166
- Frova C (2003) The plant glutathione transferase gene family: genomic structure, functions, expression and evolution. *Physiol Plant* 119:469–479
- Frova C (2006) Glutathione transferases in the genomics era: new insights and perspectives. *Biomol Eng* 23:149–169
- Gouet P, Courcelle E, Stuart DI, Metz F (1999) ESPript: multiple sequence alignments in PostScript. *Bioinformatics* 15:305–308
- Hayes JD, Pulford DJ (1995) The glutathione S-transferase supergene family: regulation of GST and the contribution of the isoenzymes to cancer chemoprotection and drug resistance. *Crit Rev Biochem Mol Biol* 30:445–600
- Hayes JD, Flanagan JU, Jowsey IR (2005) Glutathione transferases. *Annu Rev Pharmacol Toxicol* 45:51–88
- Hou L, Honaker MT, Shireman LM, Balogh LM, Roberts AG, Ng K, Nath A, Atkins WM (2007) Functional promiscuity correlates with conformational heterogeneity in A-class glutathione S-transferases. *J Biol Chem* 282:23264–23274
- Ivanetich KM, Goold RD, Sikakana CNT (1990) Explanation of the non-hyperbolic kinetics of the glutathione S-transferases by the simplest steady-state random sequential Bi Bi mechanism. *Biochem Pharmacol* 39:1999–2004
- Jakobson I, Warholm M, Mannervik B (1979) The binding of substrates and a product of the enzymatic reaction to glutathione S-transferase A. *J Biol Chem* 254:7085–7089
- Karavangeli M, Labrou NE, Clonis YD, Tsaftaris A (2005) Development of transgenic tobacco plants overexpressing maize glutathione S-transferase I for chloroacetanilide herbicides phytoremediation. *Biomol Eng* 22:121–128
- Koeplinger KA, Zhao Z, Peterson T, Leone JW, Schwende FS, Heinrikson RL, Tomasselli AG (1999) Activated sulfonamides are cleaved by glutathione-S-transferases. *Drug Metab Dispos* 27:986–991
- Kolm RH, Danielson UH, Zhang Y, Talalay P, Mannervik B (1995) Isothiocyanates as substrates for human glutathione transferases: structure–activity studies. *Biochem J* 311:453–459
- Labrou NE, Mello LV, Clonis YD (2001) Functional and structural roles of the glutathione-binding residues in maize (*Zea mays*) glutathione S-transferase I. *Biochem J* 358:101–110

- Labrou NE, Kotzia GA, Clonis YD (2004) Engineering the xenobiotic substrate specificity of maize glutathione S-transferase I. *Protein Eng Des Sel* 17:741–748
- Lamoureux GL, Rusness DG (1993) Glutathione in the metabolism and detoxification of xenobiotics in plants. In: De Kok IJ, Stulen J, Rennenberg H, Brunold C, Rauser W (eds) *Sulphur nutrition and assimilation in higher plants*. SPB Academic Publishers, Netherlands, pp 221–237
- Liebau E, Dawood KF, Fabrini R, Fischer-Riepe L, Perbandt M, Stella L, Pedersen JZ, Bocedi A, Petrarca P, Federici G, Ricci G (2009) Tetramerization and cooperativity in *Plasmodium falciparum* glutathione S-transferase are mediated by atypic loop 113–119. *J Biol Chem* 284:22133–22139
- Lo Bello M, Battistoni A, Mazzetti AP, Board PG, Muramatsu M, Federici G, Ricci G (1995) Site-directed mutagenesis of human glutathione transferase P1-1. Spectral, kinetic, and structural properties of Cys-47 and Lys-54 mutants. *J Biol Chem* 270:1249–1253
- Luthy R, Bowie JU, Eisenberg D (1992) Assessment of protein models with three-dimensional profiles. *Nature* 356:83–85
- Mannervik B, Danielson UH (1988) Glutathione transferases-structure and catalytic activity. *CRC Crit Rev Biochem* 23:283–337
- Marrs KA (1996) The functions and regulation of glutathione S transferases in plants. *Annu Rev Plant Physiol Plant Mol Biol* 47:127–158
- McGonigle B, Keeler SJ, Lau SM, Koeppe MK, O’Keefe DP (2000) A genomics approach to the comprehensive analysis of the glutathione S-transferase gene family in soybean and maize. *Plant Physiol* 124:1105–1120
- McManus G, Costa M, Canals A, Coll M, Mantle TJ (2011) Site-directed mutagenesis of mouse glutathione transferase P1-1 unlocks masked cooperativity, introduces a novel mechanism for ‘ping pong’ kinetic behaviour, and provides further structural evidence for participation of a water molecule in proton abstraction from glutathione. *FEBS J* 278:273–281
- Meyer DJ, Crease DJ, Ketterer B (1995) Forward and reverse catalysis and product sequestration by human glutathione S-transferases in the reaction of GSH with dietary aralkyl isothiocyanates. *Biochem J* 306:565–569
- Oakley AJ (2005) Glutathione transferases: new functions. *Curr Opin Struct Biol* 15:716–723
- Patskovsky YV, Patskovska LN, Listowsky I (2000) The enhanced affinity for thiolate anion and activation of enzyme-bound glutathione is governed by an arginine residue of human Mu class glutathione S-transferases. *J Biol Chem* 275:3296–3304
- Pemble SE, Wardle AF, Taylor JB (1996) Glutathione S-transferase class Kappa: characterization by the cloning of rat mitochondrial GST and identification of a human homologue. *Biochem J* 319:749–754
- Petterson EF, Goddard TD, Huang CC, Couch GS, Greenblatt DM, Meng EC, Ferrin TE (2004) UCSF Chimera—a visualization system for exploratory research and analysis. *J Comput Chem* 25:1605–1612
- Reinemer P, Prade L, Hof P, Neufeind T, Huber R, Zettl R, Palme K, Schell J, Koelln I, Bartunik HD, Bieseler B (1996) Three-dimensional structure of glutathione S-transferase from *Arabidopsis thaliana* at 2.2 Å resolution: structural characterization of herbicide-conjugating plant glutathione S-transferases and a novel active site architecture. *J Mol Biol* 255:289–309
- Ricci G, Lo Bello M, Caccuri AM, Pastore A, Nuccetelli M, Parker MW, Federici G (1995) Site-directed mutagenesis of human glutathione transferase P1-1. Mutation of Cys-47 induces a positive cooperativity in glutathione transferase P1-1. *J Biol Chem* 270:1243–1248
- Sali A, Blundell TL (1993) Comparative protein modelling by satisfaction of spatial restraints. *J Mol Biol* 234:779–815
- Sappl PG, Carroll AJ, Clifton R, Lister R, Whelan J, Harvey Millar A, Singh KB (2009) The Arabidopsis glutathione transferase gene family displays complex stress regulation and co-silencing multiple genes results in altered metabolic sensitivity to oxidative stress. *Plant J* 58:53–68
- Segel IH (1975) *Enzyme kinetics*. Wiley, New York, pp 460–461
- Sheehan D, Meade G, Foley VM, Dowd CA (2001) Structure, function and evolution of glutathione transferases: implications for classification of non-mammalian members of an ancient enzyme superfamily. *Biochem J* 360:1–16
- Sippl MJ (1993) Recognition of errors in three-dimensional structures of proteins. *Proteins* 17:355–362
- Skopelitou K, Muleta AW, Pavli O, Skaracis GN, Fletmetakis E, Papageorgiou AC, Labrou NE (2011) Overlapping protective roles for glutathione transferase gene family members in chemical and oxidative stress response in *Agrobacterium tumefaciens*. *Funct Integr Genomics* (in press)
- Spadaro D, Yun BW, Spoel SH, Chu C, Wang YQ, Loake GJ (2010) The redox switch: dynamic regulation of protein function by cysteine modifications. *Physiol Plant* 138:360–371
- Thompson ST, Stellwagen E (1976) Binding of Cibacron blue F3GA to proteins containing the dinucleotide fold. *Proc Natl Acad Sci USA* 73:361–365
- Thompson JD, Higgins DJ, Gibson TJ (1994) CLUSTALW: improving the sensitivity of progressive multiple sequence alignment through sequence weighting, position-specific gap penalties and weight matrix choice. *Nucleic Acids Res* 22:4673–4680
- Urano K (1982) Onecide, a new herbicide fluzifop-butyl. *Jpn Pestic Inf* 41:28–31